Spectral indices and multi-temporal change image detection algorithms for burned area extraction in the Brazilian Cerrado

Arturo Emiliano Melchiori[1]
Pietro de Almeida Cândido[1]
Renata Libonati[1]
Fabiano Morelli[1]
Alberto W. Setzer[1]
Silvia Cristina de Jesus[1]
Leila Maria Garcia Fonseca[2]
Thales Sehn Körting[2]

Instituto Nacional de Pesquisas Espaciais - INPE
Caixa Postal 515 - 12227-010 - São José dos Campos - SP, Brasil
[1] Centro de Previsão de Tempo e Estudos Climáticos
{emiliano.melchiori; pietro.candido; renata.libonati; alberto.setzer;fabiano.morelli}@cptec.inpe.br
silvia.jesus@inpe.br
[2] Divisão de Processamento de Imagens
{Leila; tkorting}@dpi.inpe.br

Abstract. Accurate burned area information is required and of particular interest for the scientific communities dealing with land use and climate changes. This paper presents the results of a separation index M in the comparison of seven spectral indices for automatic extraction of burned area scars, tested with Landsat TM in the Cerrado (savannah) biome of Brazil. A series of six TM scenes (path/row: 221/067) covering the period of July to September 2010 was used. Input images were accepted with cloud cover up to 10%, and the maximum period of time between consecutive scenes was up to 1 month. Burn scar maps were produced manually for intersection with the extraction of burned and non-burned areas from the indices. Several spectral indices were calculated: Normalized Difference Vegetation Index (NDVI), Normalized Burn Ratio Long SWIR Variation (NBRL), Normalized Burn Ratio Short and Long SWIR Variation (NBRSL), MODIS Burned Area Index Short SWIR Variation (BAIMS), MODIS Burned Area Index Long SWIR Variation (BAIML), Mid Infrared Burned Index (MIRBI) and W Index, and different approaches for multi-temporal change detection were evaluated: difference, normalized difference, relative difference and a variation of the delta difference. Results show a strong performance of the NBRSL, NDVI, NBRL, W and MIRBI indices, in combination with the variation of the delta difference. The results obtained can be considered as an important part in the development of automatic burned area extraction tools for the Cerrado region, particularly for conservation areas were sudden changes are commonly associated with fires.

Keywords: burned area, spectral indices, separation index, Landsat, Cerrado

1. Introduction

The Brazilian Cerrado extends over 2,000,000 Km^2 occupying almost a fourth of the country's territory and is considered the most bio-diverse savannah of the world. Deforestation already reduced this biome to at least 50%, and if degradation is also considered, this value increases significantly (KLINK and MACHADO, 2005). Conservation areas account only for 8.2% of the Cerrado, and an additional 4.4% are preserved as indigenous territories (MMA, 2014a; KLINK and MACHADO, 2005). The study area is located in the Jalapão region, in the northeast portion of central Brazil, comprising the largest and more important conservation areas of the Cerrado biome – see Figure 1. Its elevation ranges from 150 m to 950 m, and the climate in the region is hot semi-humid, with a pronounced dry season. Rains are concentrated in October-to-April, the so-called summer season, with up to 600 mm of average precipitation in the rainiest trimester, while winter, from May through September, may accumulate as little as 25 mm. Soils have a large

proportion of quartz sands, almost 50%; the population density is below 2.5 inhabitants/km^2 (INMET, 2014, SEPLAN, 2013; PRADO DOS SANTOS et al, 2011).

Increasing efforts are being made by federal and state agencies in this region to control deforestation processes and anthropic vegetation fires (MMA, 2012; MMA, 2014b). During the severe drought period of 2010, 60% of all fires in the Cerrado biome were detected in the Jalapão ecologic corridor. Remote sites and fire brigade's limited operational conditions contribute to an inefficient control of fires. The total fire pixel detections by Projeto Queimadas of INPE, Brazil (INPE, 2014), accounts for 83,575 events in the period 2004-2013, with an annual mean of 8,357 (CÂNDIDO, 2014); this value refers to multiple satellite platforms, when a unique fire event might have simultaneous detections from more than one satellite. Our study area is contained in the Landsat TM scene path/row 221/067, and Figure 1 shows it within the context of the South American continent and the Cerrado biome.
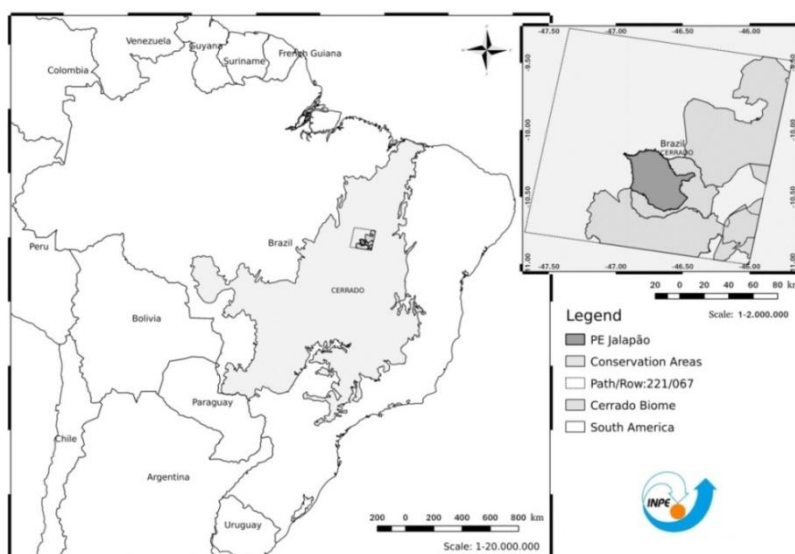

Figure 1 – Location of the study area in the Brazilian Cerrado.

Landsat TM sensor images have been widely used for precise mapping of burned scars due to its 30 meters spatial resolution in both visible and infrared channels (STROPPIANA *et al*, 2012). While temporal resolution might be adequate for multi-temporal mapping in ideal atmospheric conditions, the occasional presence of clouds and cloud shadows over the study region impair the regularity of the temporal series, even causing its interruption.

Most of the spectral indices evaluated in this work have a long history of use, some of them exclusively developed for burned area extraction (BASTARRIKA et al, 2011). Multi-temporal image change detection is a commonly used tool to accounting for changes in ecosystems (MILLER and THODE, 2007).

The objective of this work is to test a procedure for analysing and selecting automatic burned area extraction tools that quantify temporal changes of land cover in sequential mid-resolution orbital imagery in different biomes.

2. Main procedure for burned area extraction and comparison

Burned area was extracted from TM images by visual photo-interpretation and expert knowledge of the study area. As mentioned by Congalton, 1991, the accuracy of photointerpretation has been accepted as correct without any confirmation, and digital classifications are often assessed with reference to it leading to sometimes poor and unfair assessments.

Only images with total cloud cover up to 10% were used in the temporal sequence of the seven scenes of 2010 used to compare existing methods of automatic burn scar mapping; the screening was done by visual inspection. All images were downloaded from the USGS server (USGS, 2014). The high quality of their geo-processing grants their use in automatic and operational processes.

The procedures for image processing were developed in the Python 2.7.4 programming language (PYTHON, 2014), using freely available function libraries like gdal (GDAL, 2014) and numpy (NUMPY, 2014). Inter-operation among these libraries simplifies the process work flow. A routine was implemented to process the Landsat TM images and obtain the statistical evaluation of both burned scar maps and non-burned area for the study region. This program handles the decompression of downloaded data, generation of a layer stack, cropping, conversion to TOA reflectance, evaluation of the spectral indices, multi-temporal change detection, intersection with reference data, statistical measurements, evaluation of a separation index, and also automatically saving the obtained results. A diagram showing the entire process is shown in Figure 2.
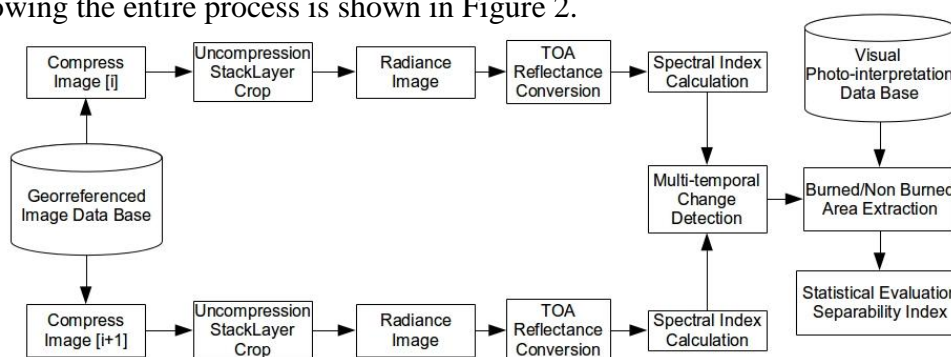
Figure 2 – Flow diagram of the process developed.

The following indices were considered: Normalized Difference Vegetation Index (NDVI) (GITELSON et al, 1996); Normalized Burn Ratio Long SWIR Variation (NBRL) (BASTARRIKA et al, 2011; KEY & BENSON, 2006); Normalized Burn Ratio Short and Long SWIR Variation (NBRSL); MODIS Burned Area Index Short SWIR Variation (BAIMS) (MARTÍN et al, 2005); MODIS Burned Area Index Long SWIR Variation (BAIML) (MARTÍN et al, 2005), W Index (LIBONATI et al, 2011) and Mid Infrared Burned Index (MIRBI) (TRIGG and FLASSE, 2001). They were calculated using sensor reflectance data, and conversion from digital numbers to TOA reflectance followed Chander et al, 2009.

$$NDVI = \frac{\rho_{NIR} - \rho_{RED}}{\rho_{NIR} + \rho_{RED}} \tag{1}$$

$$NBRL = \frac{\rho_{NIR} - \rho_{SWIRL}}{\rho_{NIR} + \rho_{SWIRL}} \tag{2}$$

$$NBRSL = \frac{\rho_{SWIRS} - \rho_{SWIRL}}{\rho_{SWIRS} + \rho_{SWIRL}} \tag{3}$$

$$BAIMS = \frac{1}{(\rho_{NIR} - \rho_{CNIR})^2 + (\rho_{SWIRS} - \rho_{CSWIRS})^2} \tag{4}$$
$$\rho_{CNIR} = 0.05, \rho_{CSWIRS} = 0.2$$

$$BAIML = \frac{1}{(\rho_{NIR} - \rho_{CNIR})^2 + (\rho_{SWIRL} - \rho_{CSWIRL})^2} \tag{5}$$
$$\rho_{CNIR} = 0.05, \rho_{CSWIRL} = 0.2$$

$$W = \overline{(\varepsilon - \varepsilon\_A)^2 + (\gamma - \gamma\_A)^2} \qquad (6)$$

$$\gamma = \overline{\rho_{SWIRL} - \rho_{SWIRL0}}^{\;2} + \overline{\rho_{NIR} - \rho_{NIR0}}^{\;2}$$
$$\varepsilon = \rho_{SWIRL} - \rho_{NIR}$$
$$\gamma\_A = 0$$
$$\varepsilon\_A = \rho_{SWIRL0} - \rho_{NIR0}$$
$$\rho_{SWIRL0=0.24}$$
$$\rho_{NIR0=0.05}$$

$$MIRBI = 10 \times \rho_{SWIRL} - 9.8 \times \rho_{SWIRS} \qquad (7)$$

To evaluate the change between consecutive pairs of images in time, pre-fire (*PrFC*) and post-fire conditions (*PsFC*) were used. Different multi-temporal change detection methods were considered: Difference (DIF) (KEY and BENSON, 2005), Delta difference relative to pre-fire condition (dDIFPre) (MILLER and THODE, 2007, MELCHIORI, 2014), Relative version of delta difference (MILLER and THODE, 2007) and Normalized difference (NorDIF):

$$Dif = PrFC - PsFC \qquad (8)$$

$$dDIF_{PRE} = \frac{(PrFC - PsFC)}{abs(PrFC)} \qquad (9)$$

$$RdDIF = \frac{(PrFC - PsFC)}{abs(\frac{PrFC}{1000})}) \qquad (10)$$

$$NorDIF = \frac{(PrFC - PsFC)}{(PrFC + PsFC)} \qquad (11)$$

Intersection of the manually extracted burned area maps with the resulting images produced two sets of data: the burned scars, and the remaining non-burned area. An example of the extraction is shown in Figure 3 for the W index image. The non-burned areas are shown in the left image by the different shades of green, while the burned areas are shown at the right.
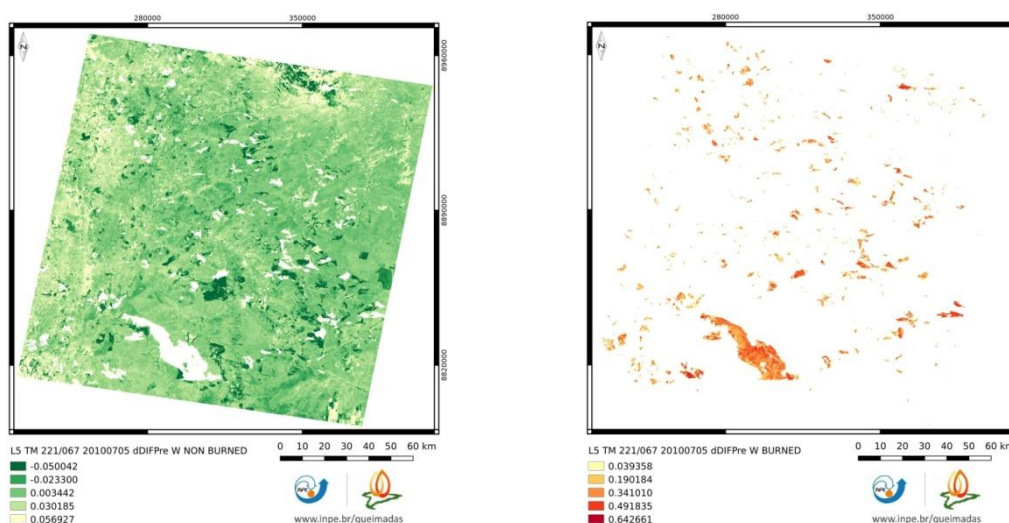

Figure 3 –Non-burned areas (left image) and burned areas (right image) for the W index.

From the two sets, non-burned (NB) and burned (B), and using only reference data, the mean (μ) and standard deviation (σ) were obtained. With them, the M separation index was evaluated (KAUFMAN & REMER, 1994).

$$M = \frac{\mu NB - \mu B}{\sigma NB + \sigma B}$$ (12)

Values of M higher than 1 indicate good separation capabilities of the evaluated index.

Divergences were found in the calculation of dDIFPre, just as mentioned by Miller and Thode, 2007, when a very small value of the index occurs in the PrFC, resulting in an extreme value of the normalized difference. These high values of change will be then translated into high values of variance, producing a non-reliable separation index. These discrepancies motivate using a median filter to smooth the images and filter these high values.

3. Results

The obtained results, with and without median filter, are shown in Figures 4, 5 and 6. The left part of each polar graph contain the separation index obtained after using a median filter of 5 pixels, indicated with a suffix .M, while the right side of each graph depicts the separation index obtained without a median filter.
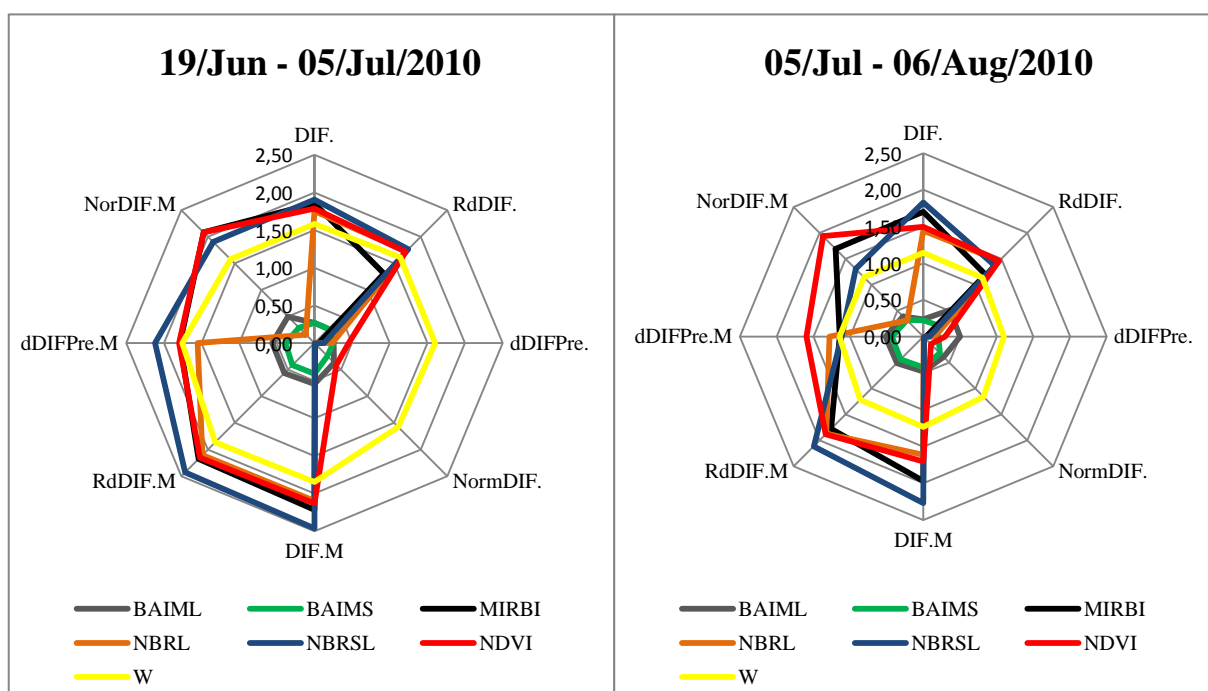

Figure 4. Polar diagrams of M according to each index and change evaluation method for the date periods: on the left, from 19/Jun–5/Jul/2010; on the right, from 05/Jul–06/Aug/2010.
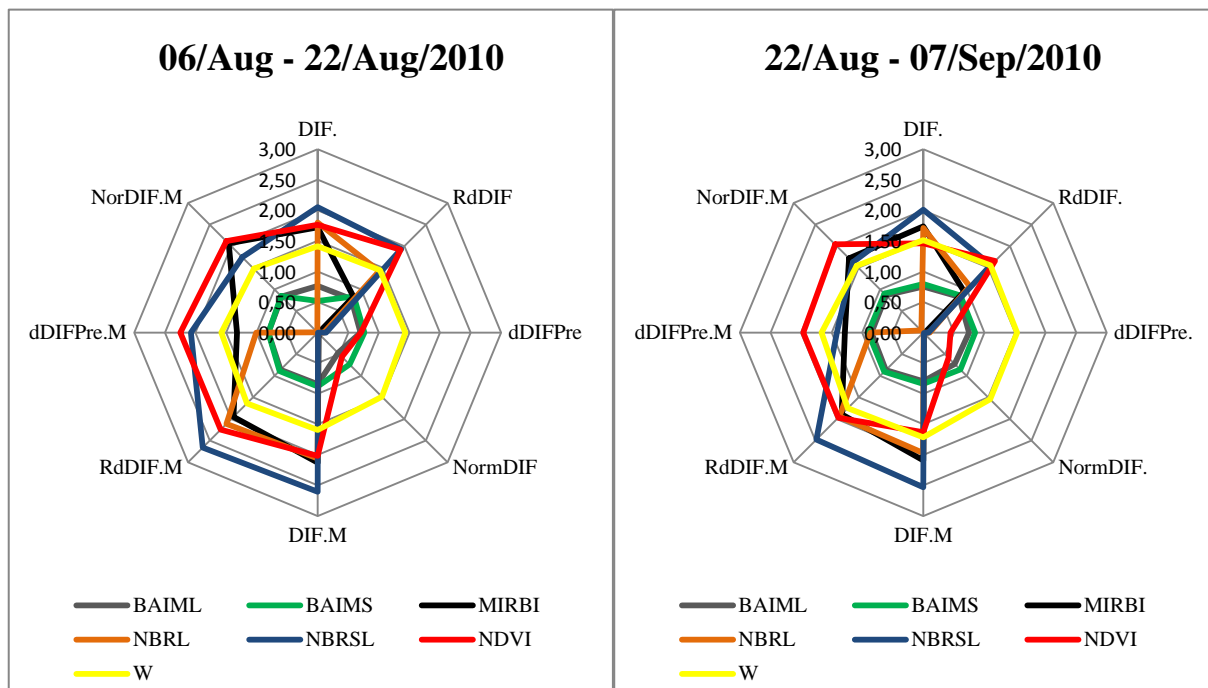
Figure 5. Polar diagrams of M according to each index and change evaluation method for the date periods: on the left, from 06/Aug–22/Aug/2010 on the right, from 22/Aug–07/Sep/2010.
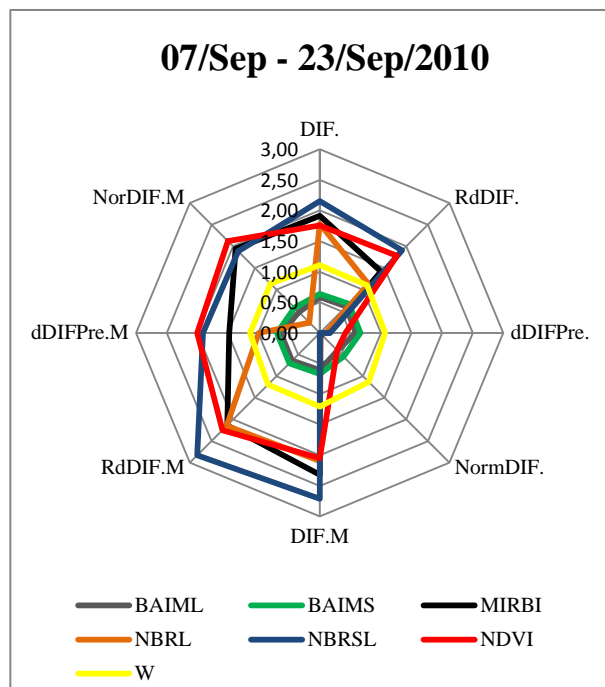

Figure 6. Polar diagram of M according to each index and change evaluation method for the period of 07/Sep - 23/Sep/2010.

4. Conclusions

From the presented results it is possible to observe the different separation capabilities of existing indices and change detection algorithms for the extraction of burned areas in the Brazilian Cerrado. Among the spectral indices, the best separation capabilities are found with the NBRSL, NDVI and W indices, showing an almost constant separation capability across the imagery used. NBRL and MIRBI also present a good separation capability, although lower than the three mentioned indices. It is worth to point that W, NBRSL, NBRL and MIRBI indices use a long SWIR band (2.08-2.35μm) which is not available in many orbital sensors. A future study may involve the short SWIR (1.55-1.75 μm) variation of the NBR index to evaluate its performance. BAIMS and BAIML presented the worst separation capability for the whole series, meaning that they should not be indicated for burned area detection at the Jalapão region.

Within the change detection algorithms, the highest value is obtained with the RdDIF approach followed by the absolute difference, both after the median filter. Before the use of the median filter, the best separation capabilities result from the combination of the difference and the delta difference with the NBRSL index. The W index presented the best separation capabilities for the dDIFPre and NormDIF methods. Concerning the absolute difference, Miller and Thode (2007) conclude that it may not be adequate when extracting scars in heterogeneous landscapes because of the need of diverse thresholds to consider the different land cover changes when affected by fire. An indication of change relative to the pre-fire condition can be understood as a percentage of the damage produced by the fire within a more natural idea of the concept of change.

The results here described identified the effect of the median filter in the change detection algorithms. Those change detection algorithms that have the PrFC in the denominator did benefit from the smoothing operation of the filter which effectively eliminates outliers in the images.

The comparative procedure presented is recommended in the analyses and selection of automatic burned area extraction tools that quantify temporal changes of land cover in sequential mid-resolution orbital imagery in different biomes.

Acknowledgments

References

Bastarrika. A.; Chuvieco, E. Martín, M.P. Mapping burned areas from Landsat TM/ETM+ data with a two phase algorithm: Balancing omission and commission errors. Remote Sensing of Environment. 2011. 105:1003-1012

Cândido, P.A. Monitoramento de Queimadas e Incêndios na Região do Parque Estadual do Jalapão em 2004 e 2013. 2014. Relatório Atividades GIZ, Internal Report.

Chander, G.; Markham, B.L.; Helder, D.L. Summary of current radiometric calibration coefficients for Landsat MSS, TM, ETM+ and EO-1 ALI sensors. Remote Sensing of Environment. 2009. 113:893-903

Congalton, R.G. A Review of Assessing the Accuracy of Classifications of Remotely Sensed Data. Remote Sensing of Environment. 1991. 37:35-46

Gdal. Available in: <www.gdal.org> Access on: 14.Oct.2014

Gitelson, A.A.; Kaufman, Y.J.; Merzlyak, M.N. Use of a Green Channel in Remote Sensing of Global Vegetation from EOS-MODIS. Remote Sensing of Environment. 1996. 58:289-298.

INMET. Instituto Nacional de Meteorologia, Climatologia da Faixa Normal – dados de 1961-2010. http://www.inmet.gov.br/portal/index.php?r=clima/faixaNormalPrecipitacaoTrimestral. Access on 14/July 2014.

INPE – Instituto Nacional de Pesquisas Espaciais – Projeto Queimadas. 2014. <http://www.inpe.br/queimadas> Access on 14/July/2014.

Kaufman, Y.J. & Remer, L.A. (1994). Detection of forest using mid-IR reflectance: an application for aerosol studies. IEEE Transactions on Geoscience and Remote Sensing, 32, 672-683

Key, C.H. Benson, N.C. Landscape assessment (LA): Sampling and Analysis Methods – Remote Sensing of severity, the Normalized Burn Ratio. USDA Forest Service Gen. Tech. Rep. RMRS-GTR-164-CD. 2006. LA1-LA5.

Klink, C. and Machado, R.B. Conservation of the Brazilian Cerrado. Conservation Biology, 19 (3), 707-713, 2005.

Libonati, R., DaCamara, C.C., Pereira, J.M.C. and Peres, L.F. On a new coordinate system for improved discrimination of vegetation and burned areas using MIR/NIR information. Remote Sensing of Environment. 2011. 115: 1464-1477

Martín, M. P., Gómez, I., & Chuvieco, E. (2005). Performance of a burned-area index (BAIM) for mapping Mediterranean burned scars from MODIS data. In J. Riva, F. Pérez-Cabello, & E. Chuvieco (Eds.), Proceedings of the 5th International Workshop on Remote Sensing and GIS applications to Forest Fire Management: Fire Effects Assessment (pp. 193−198). Paris: Universidad de Zaragoza, GOFC-GOLD, EARSeL.

Melchiori, A.E. Algoritmo digital para estimar áreas queimadas em imagens de media resolução da região do Jalapão. 2014. Relatório Atividades GIZ, Internal Report.

MMA – Ministério do Meio Ambiente. Plano de Ação para Prevenção e Controle do Desmatamento e das Queimadas no Cerrado, Brasília, 2010. <http://www.mma.gov.br/estruturas/201/_arquivos/ppcerrado_201.pdf> Access on 14/July/2014.

MMA – Ministério do Meio. Ambiente. Contra o fogo no Cerrado. 2012. <http://www.mma.gov.br/informma/item/8482-contra-o-fogo-no-cerrado> Access on 14/July/2014.

MMA – Ministério do Meio. Ambiente. O Bioma Cerrado. <http://www.mma.gov.br/biomas/cerrado> Access on 15/July/2014.

Miller, J.D.; Thode, A.E. Quantifying burn severity in a heterogeneous landscape with a relative version of the delta Normalized Burn Ratio (dNBR). Remote Sensing of Environment. 2007. 109:66-80.

Prado dos Santos, R.; Crema, A.; Szmuchrowski, M.A.; Asado, K. Kawaguchi, M. Atlas do Corredor Ecológico da Região do Jalapão. 2011. Instituto Chico Mendes de Conservação de Biodiversidade. Versão Digital.

Numpy. Available on: <www.numpy.org> Access on: 14.Oct.2014

Python. Available on: <www.python.org> Access on: 14.Oct.2014

SEPLAN – Secretaria de Planejamento e Meio ambiente. Plano de Manejo do Parque Estadual do Jalapão, Palmas, TO, 132 pp. 2003.

Stroppiana, D.; Bordogna, G.; Carrara, P.; Boschetti, M.; Boschetti, L.; Brivio, P.A. A method for extracting burned áreas from Landsat Tm/ETM+ images by soft aggregation of multiple spectral indices and a region growing algorithm. ISPRS Journal of Photogrammetry and Remote Sensing. 2012. 69:88-102.

Trigg, S., & Flasse, S. (2001). An evaluation of different bi-spectral spaces for discriminating burned shrub-savannah. International Journal of Remote Sensing, 22, 2641−2647

USGS – United States Geological Survey. 2014. <http://www.earthexplorer.usgs.gov>